IJETST- Volume||01||Issue||07||Pages 1015-1022||September||ISSN 2348-9480 2014

Open access Journal International Journal of Emerging Trends in Science and Technology

Modular Bi-Directional Power Flow Converter for Multiple Renewable Energy Sources

Authors

D. John Sundar[1], K.R. Shanmugavadivu[2], G.Padmavathi[3]

[1]Agni College of Technology, Chennai, Email: *johnsundar.me@gmail.com*
[2]Agni College of Technology, Chennai, Email: *pradikshavadivu@gmail.com*
[3]Agni College of Technology, Chennai, Email: *padma_sekar06@yahoo.co.in*

ABSTRACT

This paper presents a new bidirectional dc-dc converter for renewable energy sources with a main objective of building a reliable power source with the available unreliable energy sources i.e., renewable energy sources. Compared to the traditional full and half bridge bidirectional dc-dc converters for the similar applications, the new topology has the advantages of soft switching implementation without additional devices, high efficiency and simple control. These advantages make the new converter promising for medium and high power applications especially for auxiliary power supply in fuel vehicles and power generation where the high power density, low cost, light weight and high reliability power converters are required. The bi-directional dc-dc converter is simulated using ORCAD. The circuit is simulated in the Buck & Boost mode. The simulation results coincide with the results tested experimentally on bidirectional converters. The operating principle, theoretical analysis is provided in this project. The control circuit, power circuit & driver circuit are fabricated on general purpose PCB. The experimental results coincide with the simulation results.

Keywords: *Renewable energy sources, Auxiliary power supply , dc–dc converter, fuel cell vehicle, power generation.*

1. INTRODUCTION

Multiple input energy storage elements such as batteries and ultra-capacitors are used for the storage of power from non-conventional power generating stations such as solar, wind, gas turbine, etc. These power generating stations are non-conventional since their output is not dependable at all seasons of the year. In order to reduce the risk of non dependability the power output from these stations are made to charge battery sources or ultra-capacitors through charge controllers. Battery Charge Controllers prevent the overcharging phenomena of batteries. When battery voltage rises to a preset maximum, where the battery is completely charged, the controller Automatically reduces or stops the charging rate of the battery in use. The dc sources act as input to the proposed bi-directional power flow converter. The load connected to this converter can be a continuously operating electric drive. [1],[2].

In the previous types of bi-directional power flow controllers the input source was a single unit employing a single high frequency converter. In the later stages of development of these converters led to the addition of multiple input energy sources. The design of the transformer used, to transfer power from the primary side to the secondary, in a special way has led to the inclusion of more number of input voltage sources. The proposed converter in this project employs a

control circuit to toggle between the two input voltage sources automatically when their effective value of voltage depreciates. This control was not implemented in the previous researches done and the toggling of the input voltage sources was done manually. The main objective of this bidirectional power flow converter is to build a highly reliable power source for continuously operating drives from non-conventional energy sources. The main demerit of non-conventional energy sources is that they are unreliable. This demerit causes the use of "greener" ways of power production to stagnate for implementation in real time. The bi-directional power flow converter proposed here overcomes this demerit and produces good overall efficiency.

This paper presents a new bidirectional, isolated dc–dc converter. The new converter is based on a dual half-bridge topology. Compared to the dual full-bridge topologies, it has half the component count for the same power rating with no total device rating (TDR) penalty. In addition, unified ZVS is achieved in either direction of power flow without any additional component. Therefore, a minimum number of devices is used in the proposed circuit. Also the design has less control and accessory power needs than its full-bridge competitors. All these new features allow efficient power conversion, easy control, light weight and compacted packaging [8].

2. MAIN CIRCUIT CONFIGURATION

The proposed bidirectional dc–dc converter for fuel cell applications is shown in Fig. 2. The circuit consists of an inductor on the battery side and two half-bridges each placed on each side of the main transformer. Each switching device has a small parallel capacitor for soft switching. When power flows from the low voltage side (LVS) to the high voltage side (HVS), the circuit works in boost mode to keep the HVS voltage at a desired high value. In the other direction of power flow, the circuit works in buck mode to recharge the battery from the fuel cell or from absorbing regenerated energy. The HVS switches and the low voltage side switches are MOSFETs. The arrangement of the inductor and the LVS half bridge is unique. The LVS half bridge has double functions serving as

1) A boost converter to step up voltage

2) An inverter to produce high frequency ac voltage.

The boost function is achieved by the inductor and the LVS half bridge. The LVS boost converter draws much smoother current from the load voltage source than full bridge voltage source inverter. This integrated double function provided by the LVS half bridge is advantageous over other topologies, because the primary current rating of the transformer and current stress of the LVS devices are minimized. The capacitor across each switch is a lossless snubber (or resonant capacitor) for soft switching. The transformer is used to provide isolation and voltage matching. The leakage inductance of the transformer is utilized as an interface and energy transfer element between the two voltage-source half bridge inverters: LVS and HVS half bridges. The two voltage-source half bridge inverters: LVS and HVS half bridges, each generates a square-wave voltage applied to the primary and secondary of the transformer, respectively. The amount of power transferred is determined by the phase shift of the two square-wave voltages.

The major advantages of the proposed circuit are

1) The total device rating is the same for the dual half bridge topology and the dual full bridge for the same output power.

2) Although the devices of the half-bridge are subject to twice the dc input voltage, this is an advantage in EV/HEV and fuel cell applications because the dc input voltage is very low (12 V battery).

3) The dual half bridge topology uses only half the number of devices as the full-bridge topology.

4) The LVS half bridge produces a relatively ripple-free dc current that is desirable and friendly to the low-voltage source (fuel cell or battery);

5) Current ratings (stresses) are minimized for the LVS switching devices and transformer due to the boost function of the LVS half bridge.

6) The unified soft-switching capabilities in either

direction of power flow without additional switching devices are achieved. [4]

When power flows from the LVS to the HVS, the converter works in boost mode to keep the HVS at a desired high value. In the other direction of power flow, the converter works in buck mode to charge the energy storage elements.

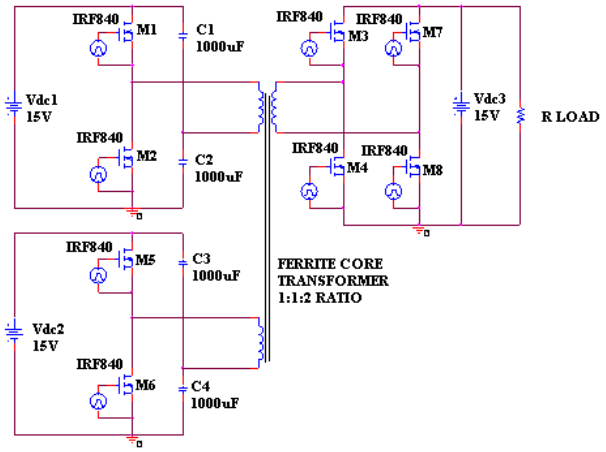

Fig 1: Proposed bi-directional dc-dc converter

The following assumptions are made to simplify the analysis.

• The inductance of L1 and L2 are large enough to maintain the currents flowing through them to be constant.

• All switching devices are considered ideal.

• The output filter capacitors C1 –C6 are large enough that V1–V6 are constant.

As shown in Fig. 3, each LVS generates a square-wave voltage (Vr12 and Vr56) on the primary side of the transformer. The HVS half-bridge generates a square-wave voltage (Vr34) on the secondary side of the transformer. The amount of power transferred is related to the phase-shift angles between the square-wave voltages. Fig. 4 illustrates the key waveforms in boost mode with the condition V1=V2=V5=V6<V3=V4.

Based on Fig. 4, the operation over one full switching cycle can be divided into six stages. The "Y" type transformer currents , and can be derived by the "Δ-Y " transformation, as shown in Fig. 3.

3. MODES OF OPERATION AND EQUIVALENT CIRCUITS

There are totally four modes of operation as explained in detail as shown below.

Boost Mode

The intervals of Fig. 10 describes the various stages of operation during one switching period in boost mode. The converter operation is repetitive in the switching cycle. One complete switching cycle is divided into thirteen steps. To aid in understanding each step, a set of corresponding annotated circuit diagrams is given in Fig. with a brief description of each step.

Forward mode-I:

During the forward mode-I or the boost mode-I of operation, the voltage source 1 is connected to the circuit since its value is well above the reference value. The split source capacitors C1, C2 plays a vital role in dividing the input voltage into two equal values i.e., 2*(Vs/2). The gate pulse to the MOSFET M1 is given first time period t1. The half bridge inverter acts appropriately and the output obtained is alternating in nature. This alternating square pulse is given as an input to the ferrite core transformer. The transformer steps up this value of voltage and is sent to the full bridge converter. Now the converter acts as a full bridge rectifier. The diodes D6 and D7 are conducting in this time period. The alternating input to the rectifier is converted in DC and is given as the input to the DC motor load. The voltage expression applying Kirchhoff's voltage law is obtained and also is linearised. The current ripple is hence obtained from the final expression substituting the known values.

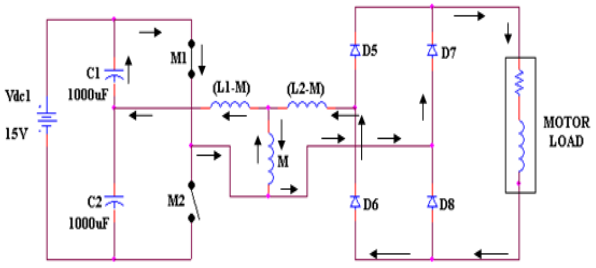

Fig 3: Equivalent circuit of forward mode I

Voltage Expression Applying Kvl To The Above Loop 1

$$\frac{V_{dc1}}{2} = (L_1 - M)\frac{di_1}{dt_1} + M\frac{di_1}{dt_1} \qquad \frac{V_{dc1}}{2} = L_1\frac{di_1}{dt_1}$$

Linearized Voltage Expression

$$\frac{V_{dc1}}{2} = L_1\frac{(\Delta I_1)}{t_1} \qquad \Delta I_1 = \frac{V_{dc1}t_1}{2L_1}$$

Substituting the values of V_{dc1}=15V, t_1=50us, L_1=5H in the above equation we get ΔI_1=0.075mA

Voltage Expression Applying Kvl To The Above Loop 2

$$0 = (L_2 - M)\frac{di_2}{dt_1} - M\frac{di_1}{dt_1} + R_L i_2 + L_1\frac{di_2}{dt_1}$$

Linearized Voltage Expression

$$0 = (L_2 - M)\frac{\Delta I_2}{t_1} - M\frac{\Delta I_1}{t_1} + R_L\Delta I_2 + L_1\frac{\Delta I_2}{t_1}$$

Substituting the values of M=3.353H, t_1=50us, L_1=5H, L_2=10H, R_L=50Ω and ΔI_1=0.075mA in the above equation we get ΔI_2=0.0189mA.

Forward mode-II:

In the forward mode-II operation the capacitor C2 delivers the energy stored in it. Now the gate pulse to the MOSFET M2 is given second time period t_2.the diodes D5 and D8 are conducting in this time period. The voltage expression applying Kirchhoff's voltage law is obtained and also is linearised. The current ripple is hence obtained from the final expression substituting the known values

Voltage Expression Applying Kvl To The Above Loop 1

$$\frac{V_{dc1}}{2} = (L_1 - M)\frac{di_3}{dt_2} + M\frac{di_3}{dt_2} \qquad \frac{V_{dc1}}{2} = L_1\frac{di_3}{dt_2}$$

Linearized Voltage Equations

$$\frac{V_{dc1}}{2} = L_1\frac{(\Delta I_3)}{t_2} \qquad \Delta I_3 = \frac{V_{dc1}t_2}{2L_1}$$

Substituting the values of V_{dc1}=15V, t_2=50us, L_1=5H we get ΔI_3=0.075mA.

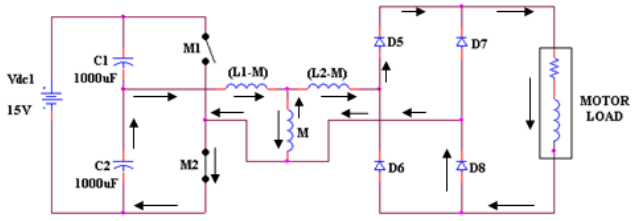

Fig 4: Equivalent circuit of forward mode II

Voltage Expression Applying Kvl To The Above Loop 2

$$0 = (L_2 - M)\frac{di_4}{dt_2} - M\frac{di_4}{dt_2} + R_L i_4 + L_1\frac{di_4}{dt_2}$$

Linearized Voltage Equations

$$0 = (L_2 - M)\frac{\Delta I_4}{t_2} - M\frac{\Delta I_4}{t_2} + R_L\Delta I_4 + L_1\frac{\Delta I_4}{t_2}$$

Substituting the values of M=3.353H, t_1=50us, L_1=5H, L_2=10H, R_L=50Ω and ΔI_3=0.075mA in the above equation we get ΔI_4=0.0189mA.

The design analysis for the voltage source 2 is similar to the analysis carried out for voltage source 1 and hence the ripple current values are also identical for the respective modes of operation for voltage source2.

Buck Mode:

Reverse mode-I:

During the reverse mode or the buck mode of operation the load side acts as the source and the source acts as the load. The gating pulses are given to the full bridge inverter module and the pulses are stopped to the half bridges. The MOSFETs M5 and M8 are triggered first and the corresponding current paths are shown in the fig. 8. The output of the inverter is a square alternating pulse and is given to the ferrite core transformer. Now the transformer steps down the voltage and is given to the half bridge network. Now the half bridge inverter acts as a rectifier and converts the available AC voltage to DC and is obtained across the source resistance Rs. The voltage expression applying Kirchhoff's voltage law is obtained and also is linearised. The current ripple is hence obtained from the final expression substituting the known values

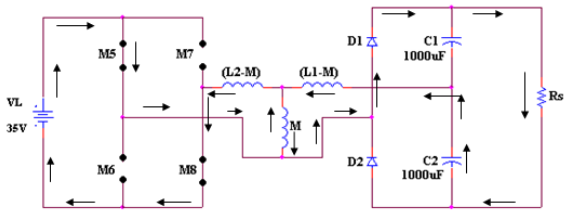

Fig 5: Equivalent circuit of reverse mode I

Voltage Expression Applying Kvl To The Above Loop 1

$$V_L = (L_2 - M)\frac{di_5}{dt_1'} + M\frac{di_5}{dt_1'}$$

Linearised Voltage Equations

$$V_L = (L_2 - M)\frac{\Delta I_5}{t_1'} + M\frac{\Delta I_5}{t_1'}$$

$$\Delta I_5 = \frac{V_L t_1'}{L_2}$$

Substituting the values for V_L=35V, t'$_1$=45us, L_2=10H we get ΔI_5=0.1575mA.

Voltage Expression Applying Kvl To The Above Loop 2

$$-M\frac{di_5}{dt_1'} - (L_1 - M)\frac{di_6}{dt_1'} + \frac{1}{C_1}\int i_6 dt_6 + R_s i_6 = 0$$

Linearised Voltage Equations

$$-M\frac{\Delta I_5}{t_1'} - (L_1 - M)\frac{\Delta I_6}{t_1'} + \frac{\Delta I_6}{C_1 f} + R_s \Delta I_6 = 0$$

Substituting the values for V_L=35V, t'$_1$=45us, L_2=10H, Rs=1kΩ and ΔI_5=0.1575mA we get **ΔI_6=0.0123mA.**

Reverse mode-II:

In this mode of operation the triggering pulses are given to the MOSFETs M6 and M7 and the corresponding current directions are shown in the fig.7&8. The voltage expression applying Kirchhoff's voltage law is obtained and also is linearised. The current ripple is hence obtained from the final expression substituting the known values.

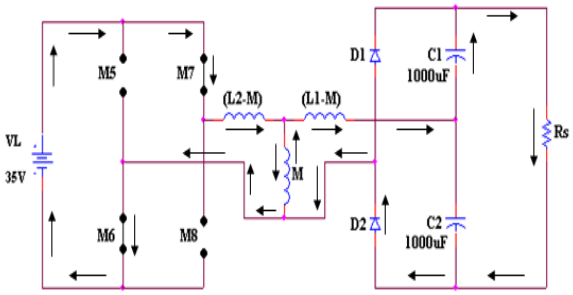

Fig 6: Equivalent circuit of reverse mode II

Voltage Expression Applying Kvl To The Above Loop 1

$$V_L = (L_2 - M)\frac{di_7}{dt_2'} + M\frac{di_7}{dt_2'}$$

Linearised Voltage Equations

$$V_L = (L_2 - M)\frac{\Delta I_7}{t_2'} + M\frac{\Delta I_7}{t_2'} \qquad \Delta I_7 = \frac{V_L t_2'}{L_2}$$

Substituting the values of V_L=35V, t'$_2$=45us, L_2=10H we get **ΔI_7=0.1575mA.**

Voltage Expression Applying Kvl To The Above Loop 2

$$-M\frac{di_7}{dt_2'} - (L_1 - M)\frac{di_8}{dt_2'} + \frac{1}{C_1}\int i_8 dt_2' + R_s i_8 = 0$$

Linearised Voltage Equations

$$-M\frac{\Delta I_7}{t_2'} - (L_1 - M)\frac{\Delta I_8}{t_2'} + \frac{\Delta I_8}{C_2 f} + R_s \Delta I_8 = 0$$

Substituting the values for V_L=35V, t'$_2$=45us, L_2=10H, Rs=1kΩ and ΔI_7=0.1575mA we get **ΔI_8=0.0123mA.**

Gating pulses to the semiconductor devices

The pulses to the various semiconductor devices are provided with Pulse Width Modulation technique and the operating frequency chosen is 10KHz. Pulse width is calculated using a frequency of 10 kHz

$$T = \frac{1}{f}\text{sec} \qquad T = \frac{1}{10000}$$

Total time period $T = 100\mu s$

The time delay between the switching of MOSFETs is taken to be 5μs.

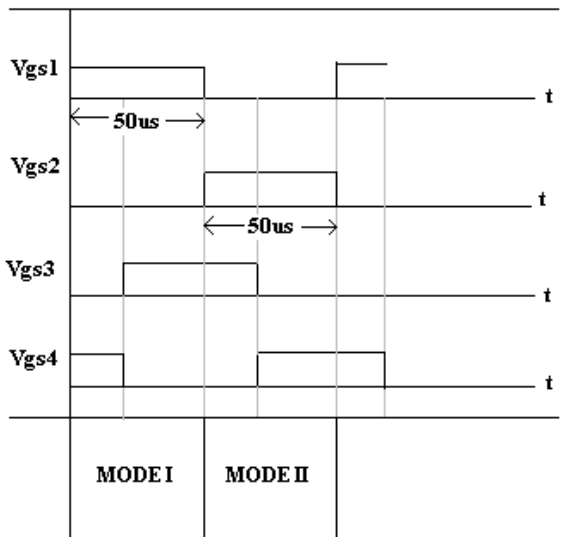

Fig.7 Gating pulses for MOSFETS in forward mode of operation

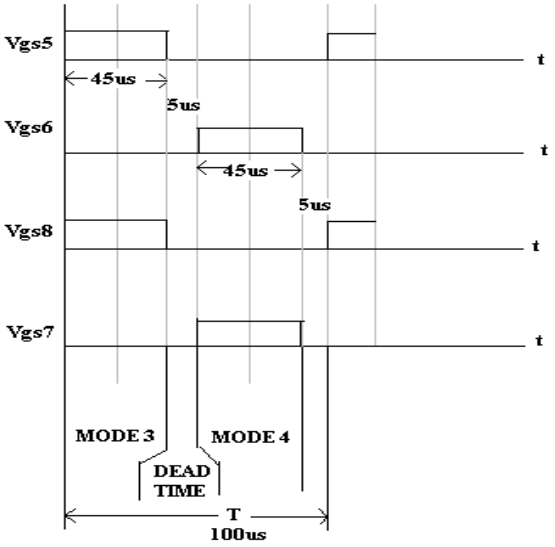

Fig.10 Gating pulses for MOSFETS in reverse mode of operation

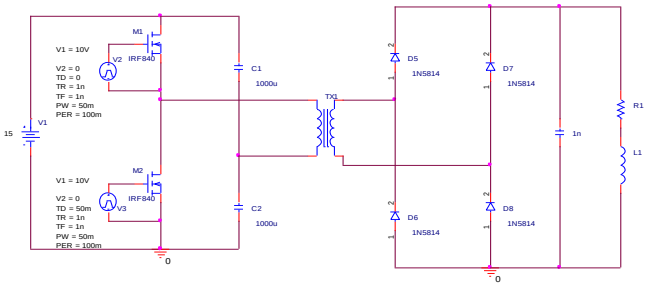

Fig 8: Simulation circuit diagram for forward modes

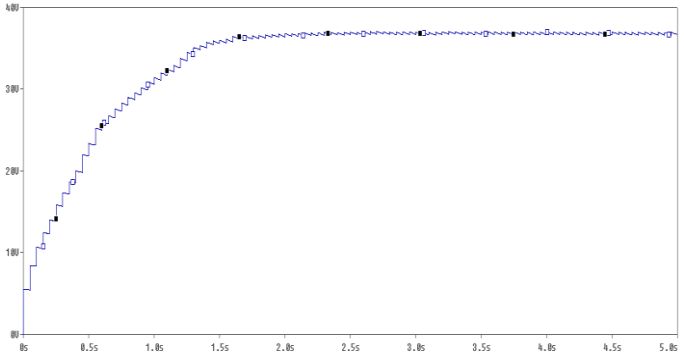

Fig 11: Output voltage waveform across the load for the forward mode operation of both the voltage sources Vdc1 and Vdc2

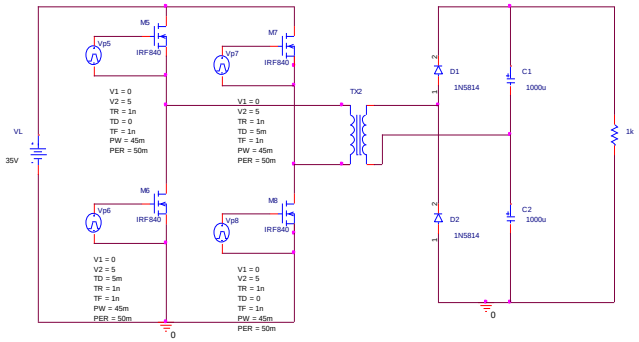

Fig 9: Simulation circuit diagram for reverse modes

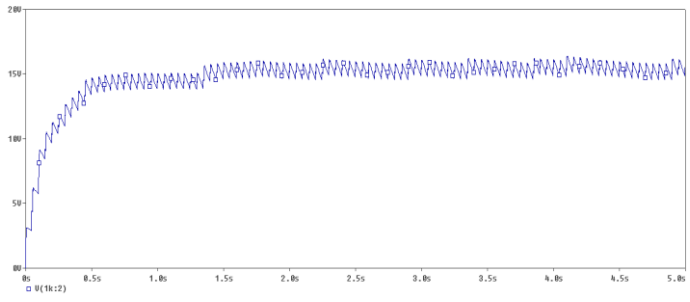

Fig 12: Output voltage waveform across the load for the reverse mode operation of both the voltage source V_{dc3}

4. CONCLUSION

The simulation of the project has been completed using the PSPICE software for a high-power-density two-input bi-directional dc–dc converter proposed as shown above. The circuit model of the multi-winding transformer, power flow control, and the soft switching conditions of the switches are provided. It is shown that two energy sources with different dc voltage levels can be combined to deliver power simultaneously in either direction. In addition, high power efficiency, high reliability, and long life-cycle operation can be achieved by the optimum power sharing between the sources.

5. REFERENCES

1. L. Solero, F. Caricchi, F. Crescimbini, O. Honorati, and F. Mezzetti, "Performance of a 10 kW power electronic interface for combined wind/PV isolated generating systems," in *Proc. IEEE Power Electron. Spec. Conf.*, 1996, pp. 1027–1032.
2. F. Caricchi, F. Crescimbini, A. Di Napoli, O. Honorati, and E. Santini, "Testing of a new DC-DC converter topology for integrated wind-photovoltaic generating systems," in *Proc. IEEE Eur. Conf. Power Electron. Appl.*, 1993, pp. 83–88.
3. H. Matsuo, T. Shigemizu, F. Kurokawa, and N. Watanabe, "Characteristics of the multiple-input DC-DC converter," in *Proc. IEEE Power Electron. Spec. Conf.*, 1993, pp. 115–120.
4. H. Matsuo, K. Kobayashi, Y. Sekine, M. Asano, and L. Wenzhong, "Novel solar cell power supply system using the multiple-input DC-DC converter," in *Proc. IEEE Int. Telecommun. Energy Conf.*, 1998, pp. 797–802.
5. Y. M. Chen, Y. C. Liu, F. Y. Wu, and T. F. Wu, "Multi-input DC/DC converter based on multiwinding transformer for renewable energy application," *IEEE Trans. Ind. Appl.*, vol. 38, no. 4, pp. 1096–1104, Jul./ Aug. 2002.
6. L. Solero, A. Lidozzi, and J. A. Pomilio, "Design of multiple-input power converter for hybrid vehicles," *IEEE Trans. Power Electron.*, vol. 20, no. 5, pp. 1007–1016, Sep. 2005.
7. H. Tao, A. Kotsopoulos, J. L. Duarte, and M. A. M. Hendrix, "Multiinput bidirectional dc-dc converter combining DC-Link and magneticcoupling for fuel cell systems," in *Proc. IEEE IAS Annu. Meeting Conf.*, 2005, pp. 2021–2028.
8. F. Z. Peng, H. Li, G.-J. Su, and J. Lawler, "A new ZVS bi-directional dc-dc converter for fuel cell and battery applications," *IEEE Trans. Power Electron.*, vol. 19, no. 1, pp. 54–65, Jan. 2004.

Author Profiles

D.John Sundar received the Bachelor and Master of Engineering degrees from Anna University Chennai in the year 2007 and 2010 respectively. His main area of research includes Grid Integration of Renewable Energy Sources, Photovoltaic Converters/Inverters and Signal processing and analysis in Electrical Power System. He is currently a Research Scholar at Anna University Chennai. Presently he works as an Assistant Professor in the Department of Electrical and Electronics Engineering at Agni College of Technology, Thalambur, Chennai, Tamil Nadu.

K.R.Shanmugavadivu received the Bachelor and Master of Engineering degrees from Anna University Chennai in the year 2006 and 2010 respectively. Her main area of research includes Grid Integration of Renewable Energy Sources, Multilevel Converters for low power applications. She is currently a Research Scholar at Anna University Chennai Presently she works as an Assistant Professor in the Department of Electrical

and Electronics Engineering at Agni College of Technology, Thalambur, Chennai, Tamil Nadu.

G.Padmavathi received the Bachelor and Master of Engineering degrees from Anna University Chennai in the year 2007 and 2009 respectively. Her main area of research includes Grid Integration of Renewable Energy Sources, Image processing using Extended Kalman Filter. Presently she works as an Assistant Professor in the Department of Electrical and Electronics Engineering at Agni College of Technology, Thalambur, Chennai, Tamil Nadu.